

Optimum Design and FEA of a Hybrid Parallel-deployable Structure-based 3-DOF Multi-gripper Translational Robot for Field Pot Seedlings Transplanting

Samy F. M. Assal^{1,2} and Isaac Ndawula¹

¹*Department of Mechatronics and Robotics Engineering,*

Egypt – Japan University of Science and Technology (EJUST), Egypt

²*On leave: Department of Production Engineering and Mechanical Design,*

Faculty of Engineering, Tanta University, Egypt

Keywords: Transplanting Robot, Multi-gripper, Optimum Design, Pot Seedlings Transplanting, Hybrid Parallel-Deployable Structure.

Abstract: Pot seedlings transplanting is an activity in the agricultural production industry. In its manual level, it is a time consuming, labour intensive, costly activity with low transplanting rate, uneven plant distribution and low degree of accuracy. So, in this paper, a novel partially decoupled 3-DOF multi-gripper pot seedlings transplanting robot is proposed to be used in the open agricultural field to increase the transplanting rate. The proposed robot is composed of two identical 2-DOF Diamond Delta robots, 1-DOF scissor mechanism and belt conveyor. Delta robot is a high speed parallel robot that is used to control the grippers in the X-Z plane while the scissor mechanism is a deployable structure that is worked in the multi-gripper and used to control the grippers in Y direction. Different kinematic and design aspects are considered; namely, the kinematic analysis and the optimum design as well as the finite element analysis in the most critical loading configuration are carried out. A unified frame work for the optimum dimensional synthesis for a prescribed workspace with force transmission and singularity avoidance constraints is developed for the optimal dimensions of the design parameters. The proposed robot is shown to have high transplanting rate and is safe in terms of stress and deformation.

1 INTRODUCTION

Transplanting is a crucial agricultural activity which involves the transfer of seedlings from their raising medium to the growing medium which is either in an open field or prepared beds under a greenhouse. It is carried out from the high dense trays to low dense ones in green house or to low dense distribution in the open agriculture field. The seedlings are classified as bare-root, plug and pot seedlings. Vegetable seedling transplanting, the pot seedling one, is one of major activities in vegetable production. It is still in the manual level featured as a time consuming, labour intensive, costly and inefficient task. Robotic transplanting as a special transplanting mechanization method is a remedy for such problems. Four types of robotic and automated

transplanters have been developed for such agriculture activity in literature; namely, robotic arm type, door frame type, automated transplanters for greenhouse and automated transplanters for open field in which walk behind type transplanter undergoes. Since the former type has been developed mostly in green house, it leaves the open field robotic transplanting problems unsolved.

Different robotic arm type transplanters have been developed for greenhouse. For instance, a 5-DOF robotic manipulator for transplanting pot pepper seedlings was developed in greenhouse (Hwang et al, 1986). It consisted of a gripper, pot-type mechanical planter and 8-bit microcomputer. It picks the seedling, transfers it and drops it in a guided hole of the mechanical planter. One seedling is fetched per transplanting cycle and a transplanting rate of 6 plants/min was recorded. A feasibility study

^a <https://orcid.org/0000-0002-7997-4363>

and a simulation of using Puma 560 robot to transplant bedding plants were performed (Kutz et al, 1987). The robot was used to validate the model and a transplanting productivity of 11 plants/min was achieved with a performance of 96%. Another feasibility study for the application of SCARA robot in seedlings transplanting was carried out (Tmg et al, 1990). The robot was equipped with sliding needle sensor at its gripper to ensure that each cell in the growing tray is filled. The cyclic time of seedling transplanting was from 2.60 to 3.25 sec and a transplanting of 18 to 23 seedlings/min was achieved. The performance of those serial type manipulators is not satisfactory due to the redundant DOF they have and their low transplanting rates. On the other hand, the dimensional synthesis and kinematic simulation of a 2-DOF parallel mechanism with a pneumatic gripper for greenhouse transplanting was studied (Hu, 2014). The transplanting capacity was 58 seedlings/min.

Door frame type robotic transplanters for greenhouse have been also developed. For instance, a robotic transplanter prototype that consists of automatic seedling feeding mechanism, a rank of pistons, a transverse conveyor and a rotating insert cup has been developed (Sakaue, 1996). This transplanter can operate in both greenhouse and open agricultural field with a productivity of 35 plants/min. A bedding plants' robotic transplanter that composed of a robotic manipulator with two electrical linear motors, end-effector, a conveyor and a vision system was developed (Ryu, 2001). The manipulator was used to move the end-effector to the desired working position while the vision system was used to identify empty cells and to reduce transplanting time with a success rate of 98%. A vegetable transplanting robot that consists of pot moving conveyor, planting pot conveyor, cell tray moving conveyor, transplanting device and fingers was developed in (Kang, 2012). The transplanting capacity of the developed robot was 2800 pots per hour and the rate of success was 99%. The main demerits of door frame structure robotic transplanters are the very huge size machine, work only in greenhouse and low transplanting rate.

Moreover, automated transplanters for greenhouse have been developed. For example, automatic transplanter for plug seedling that includes manipulator (a gantry-gate type arm), conveyor system for plug tray, flowerpots and four end-effectors was developed (Tian et al, 2010). The cycle time for successful transplanting is from 1.5 to 2 sec/seedling, and the transplanting productivity is from 1800 to 2400 seedlings/hr. A fully automated

greenhouse mechanical transplanter for potted tomato seedlings was presented (Jin et al, 2019). It is composed of a seedling supply mechanism, a picking mechanism composed with a gear-rod component and an eccentric-disk parallelogram planting part. The transplanting speed was between 60 and 90 seedlings/ min. A vegetable seedlings automatic conveying system was design for greenhouse application (Jin et al, 2018). It consisted of a tank wheel, storage seedlings mechanism, seedlings tray and hanging cup. The results showed success rate of 97.91% for taking an individual seedling.

Furthermore, rather than developing automated transplanters for greenhouse, a swing seedling pick up device for automatic precise field transplanter was designed and tested in field (Han et al, 1015). It consisted of an oscillating guide linkage mechanism and globoidal cam mechanism and two grippers. The transplanting productivity was 70 seedlings/min. An intelligent transplanting system for pot seedlings in field was design and implemented (Xin et al, 2018). It consisted of fixed-axis gear train and five bar as picking mechanism, conveying system, eccentric disc as planting mechanism, electric sensor for detection and identification of missing and unhealthy seedlings, the position sensor, the control system and stepper motors. The system was tested and the productivity was found to be 90 plants/min. Also, automated walk behind type transplanters have been developed for open field. Three models of riding type automated vegetable transplanters were developed (Tsuga, 2000). These prototypes consisted of 2 rows transplanting mechanism working simultaneously at productive frequency of 60 plants/row/min. A fully automated walk behind type hand tractor powered vegetable transplanter for paper pot seedlings was developed (Kumar and Raheman, 2011). It consisted of two sets of feeding conveyor, metering conveyor, seedling drop tube, furrower opener, soil covering device, an automatic feeding mechanism, a depth adjustment wheel and hitching arrangement. The transplanting rate was 32 seedlings/min with an efficiency of 85%. A two-row vegetable automated transplanter for transplanting pot seedlings in the field was developed (Dihingia et al, 2018). The transplanter was hitched to the walk-behind hand controlled tractor as the main source of power. The transplanting productivity of this transplanter was evaluated in the field and found to be 31 seedlings/min.

Form the aforementioned literature; it is considerably to highlight that, the introduced transplanters have low transplanting rate due to large

cyclic time of the transplanting as well as the plant-by-plant manner of carrying out the transplanting task; specifically, the transplanting of one seedling at a time. So, in this paper, as an extension of our work (Ndawula et al, 2018), a row-by-row pot seedling transplanter robot with low cyclic time is proposed to achieve high transplanting rate. It has multi grippers with 3-DOF translational motion. Its structure permits seedlings transplanting from high dense seedlings in a tray to low dense, equally spaced seedlings in the open agriculture field.

The rest of the paper is organized as follows. The description of the components of the proposed transplanter robot and its working principle are presented in Section 2. The kinematics, differential kinematics, singularity and workspace analyses are discussed in Section 3. The optimal dimensional synthesis is developed in Section 4. The finite element analysis (FEA) of the robot in the most critical loading condition is carried out in Section 5. Simulation results are presented in Section 6. Finally, conclusion is drawn in Section 7

2 DEVICE STRUCTURE AND WORKING PRINCIPLE

2.1 Device Structure

The proposed 3-DOF translational robot for row-by-row pot seedlings transplanting in the open agriculture field consists of three main parts as shown in Fig. 1. Two of which are two identical 2-DOF Diamond Delta robots positioned in two apart X-Z planes with respect to a fixed frame. Basically, the Diamond Delta is a 2-DOF translational planar parallel robot with fixed and moving platforms connected by two limbs. Each limb is composed of active and passive links. The moving platform of Delta robot is called end-effector. The two fixed platforms of those two Delta robots are assembled in the fixed frame of the proposed device such that they can counter translate in Y-direction using two guide way shafts that are used to ensure the smooth translational motion. A half-length right and half-length left hand ball screw (bidirectional ball screw), powered by a third servo motor, is used to translate those two symmetrically placed Delta robots in Y direction to come close or apart from each other depending on the desired motion. This ball screw is meshed with two nuts fixed to the two translating platforms of those Delta robots. The active links that are actively connected to the translating platforms of

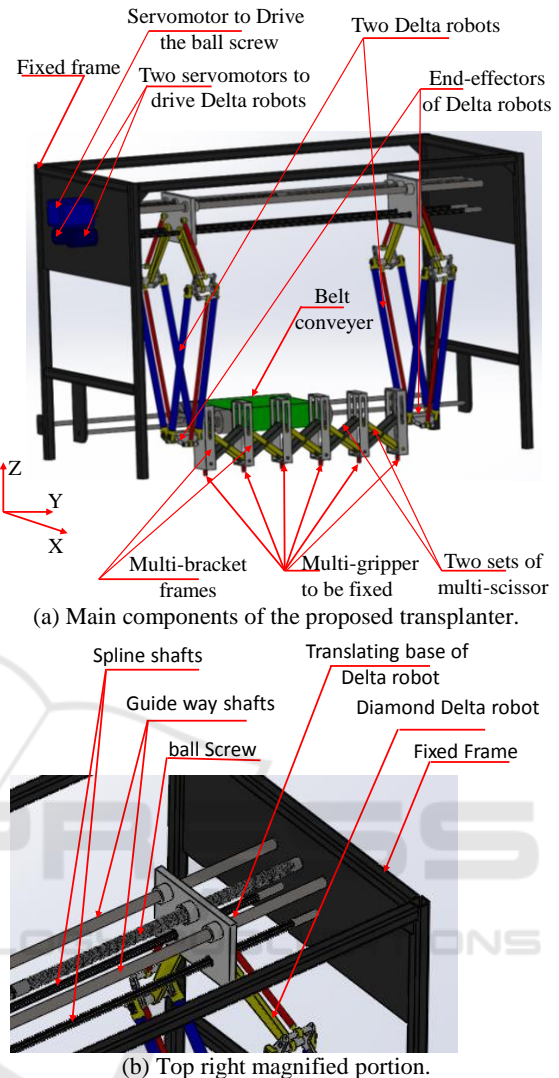


Figure 1: The proposed 3-DOF translational robotic transplanter.

those Delta robots are connected by two spline shafts which are coupled to two servo motors mounted at the top of the fixed frame as illustrated in Fig. 1. Those two spline shafts are used to mechanically synchronize the motions of the two end-effectors of the two Delta robots.

The third part of the proposed device consists of 1-DOF double planar foldable scissor mechanisms, which works in the multi-gripper, positioned in two apart Y-Z planes shown in Fig. 2. Basically, the scissor mechanism is a deployable structure with 1 DOF. The ends of the scissor mechanisms are fixed to the moving end-effectors of the two identical planar Delta robots to work as multi grippers. Those double planar foldable scissor mechanisms are connected together by multi-rectangular frames with

revolute joints and sliding grooves as shown by the 3D SolidWorks model in Fig. 2. The rectangular frames are used to keep fixed orientation of the grippers and thus restrict any orientation of the seedling grippers in any direction. This scissor mechanism keeps equal spacing between the grippers from unfolded configuration to the folded one. Thus, it allows suitable spacing in the picking up and transplanting of the seedlings. Therefore, this scissor mechanism allows row-by-row pot seedlings transplanting as many as grippers. For instance, for the standard 6×12 tray, the proposed robot can be equipped with 6 grippers. Therefore, the grippers have decoupled 3-DOF translational motion; namely, 2-DOF translational motion in X-Z plane accomplished by the parallel robots (Diamond Delta robots) and 1-DOF translational motion in Y-direction achieved by the scissor mechanism, the deployable one.

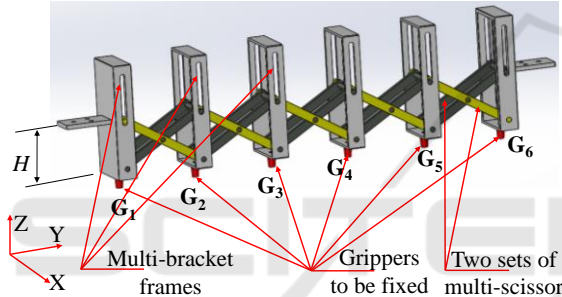


Figure 2: Two identical sets of foldable multi-scissor with multi-bracket frame.

A pot seedlings belt conveyor is another part of the device as illustrated in Fig. 1. This belt conveyor is used to carry pot seedlings tray to the appropriate position for picking up. The multi-gripper end-effector picks up pot seedlings from growing tray, holds, transfers and releases them at the time of transplanting. The proposed robot that is carried over a wheeled frame is hitched to a tractor as a source of power and its speed is synchronized with transplanting frequency of the robot.

2.2 Working Principle

The pot seedlings transplanting cycle in the field by the proposed robot occurs in three stages namely; fetching, transplanting and returning phases. The robot starts from its initial position P_0 , then follows the path $P_0-P_1-P_2$ in X-Z plane while closing gripper's spacing in Y-direction to suite the seedlings spacing on the nursery tray during seedlings fetching, as depicted in Fig. 3. At P_2 , it picks 6

seedlings in a row of the tray at once by the 6 grippers and holds them. In the transplanting phase, the robot follows the path $P_2-P_1-P_0-P_3$ while opening the scissor mechanism in Y-direction to suite the planting space in the open agriculture field. At P_3 , it releases the seedlings and drops them by gravity in the vertical orientation that is achieved by the multi-bracket frames. Then, in the returning phase, it returns to its original position P_0 following the path P_0-P_3 . This cyclic process is repeated over and over again until the operation is done. The belt conveyor ensures the steady supply of pot seedlings at the appropriate picking up position and the tractor controls column spacing of the seedlings through synchronization of motion between the tractor and proposed robot. Note that, six furrows can be opened in the agriculture field by 6 teeth shovel type furrow opener while covering the seedlings with sufficient soil and pressing the soil around the seedlings can be done by six pairs of press wheels tilted outside at the top, which is out of scope. The furrow opening as well as covering and pressing the soil around the seedlings should be synchronized with transplanting process.

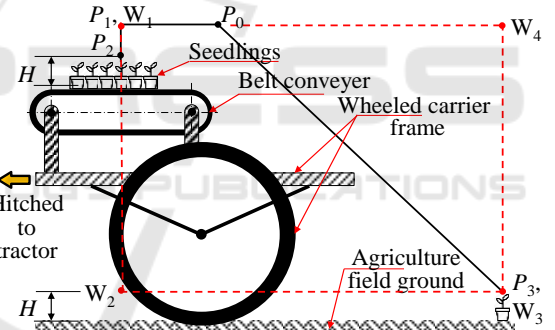


Figure 3: Seedlings transplanting cycle.

3 KINEMATIC ANALYSES

The main components of the proposed robotic transplanter to be kinematically analysed are the two 2-DOF planar Diamond Delta robots. Delta robot is a well-known positioning planar parallel manipulator that consists of a base frame and a moving frame (end-effector) as shown in Fig. 4. Those two frames are connected together by two mirror symmetrical kinematic chains. Each kinematic chain consists of two parallelograms which represent the proximal and distal links that are connected by revolute joints. The proximal link is activated by servo motor that is fixed to the fixed frame of the device through the spline shaft, while

the distal link is passive. Due to the equivalence of length of the inner and outer links of each parallelogram, Delta robot can be simplified as a 5-bar mechanism as illustrated in Fig. 4(b). The inverse kinematic of this Delta robot is of interest since it is required for the positioning control and the trajectory planning.

3.1 Inverse Kinematics

The inverse kinematics of Delta robot is to obtain the joint angle variables θ_{li} for $i=1, 2$ for the given end-effector position $P(x, z)$. For this sake, the loop closure equation of the two closed loop kinematic chains depicted in Fig. 4(b) are given as follows:

$$\mathbf{p} = e\mathbf{e}_i + l_1 \mathbf{u}_i + l_2 \mathbf{w}_i \text{ for } i=1, 2 \quad (1)$$

where $\mathbf{p} = [x \ z]^T$ is the position vector of the end-effector; \mathbf{e}_i is a unit vector directed from O to O_i while $2e$ is the centre distance between the two spline shafts that connected the active links to the two servo motors; l_1 is the proximal (active) link length while \mathbf{u}_i is a unit vector directed from O_i to A_i given as $\mathbf{u}_i = [\cos \theta_{li} \ \sin \theta_{li}]^T$, l_2 is the distal (passive) link length, while \mathbf{w}_i is a unit vector directed from A_i to P given as $\mathbf{w}_i = [\cos \theta_{2i} \ \sin \theta_{2i}]^T$. From (1), the active joint angle variables can be obtained in terms of the end-effector position as follows (Huang et al, 2004).

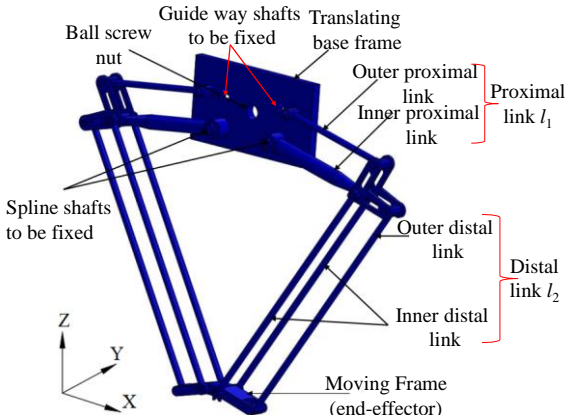
$$\theta_{li} = 2 \arctan \frac{-L_i + \text{sgn}(i)\sqrt{L_i^2 - N_i^2 + M_i^2}}{N_i - M_i} \quad \text{for } i=1, 2 \quad (2)$$

where $L_i = -2l_i z$, $M_i = -2l_i(x - \text{sgn}(i)e)$ and $N_i = x^2 + z^2 + e^2 + l_1^2 - l_2^2 - 2\text{sgn}(i)ex$, in which $\text{sgn}(i)=1$ for $i=1$, otherwise $\text{sgn}(i)=-1$

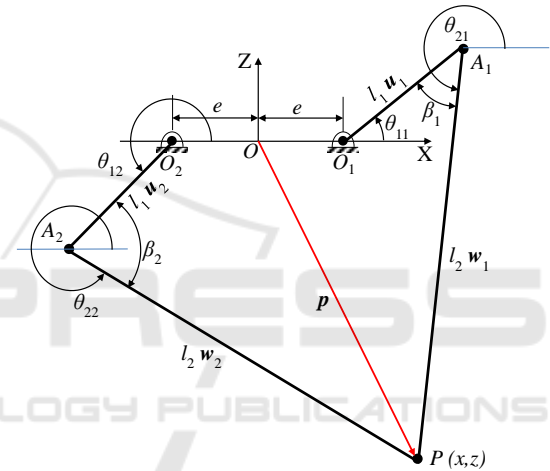
3.2 Differential Kinematics

Differentiating the loop closure equation (1) with respect to time yields velocity relation as the following

$$\dot{\mathbf{v}} = l_1 \dot{\theta}_{li} Q \mathbf{u}_i + l_2 \dot{\theta}_{2i} Q \mathbf{w}_i \text{ for } i=1, 2 \quad (3)$$



(a) SolidWork model



(b) 5-bar simplified model of Delta robot

Figure 4: The 2-DOF planar Diamond Delta robot in X-Z plane.

where $\mathbf{v} = \begin{bmatrix} \cdot & \cdot \\ x & z \end{bmatrix}^T$ is the Delta robot end-effector linear velocity vector in the X-Z Cartesian space, $Q = \begin{bmatrix} 0 & -1 \\ 1 & 0 \end{bmatrix}$ is a skew symmetric matrix. Pre-multiplying (3) by \mathbf{w}_i^T , the passive joint angles velocities $\dot{\theta}_{2i}$ for $i=1, 2$ can be eliminated and the result can be written in a matrix form as follows

$$J_2 \mathbf{v} = l_1 J_1 \dot{\theta}_1 \quad (4)$$

where J_1 and J_2 are the direct and inverse Jacobian matrices, respectively given as follows:

$$J_1 = \begin{bmatrix} \mathbf{w}_1^T Q \mathbf{u}_1 & 0 \\ 0 & \mathbf{w}_2^T Q \mathbf{u}_2 \end{bmatrix} \quad (5)$$

$$J_2 = [\mathbf{w}_1 \quad \mathbf{w}_2]^T \quad (6)$$

On the other side, the linear velocities of the grippers in the Y direction are related to the angular velocity of the ball screw. For instance, the linear velocities of gripper G_1 and G_6 shown in Fig. 2 are given as follows:

$$v_{G_1} = -v_{G_6} = \frac{L_s}{2\pi} \dot{\phi} \quad (7)$$

where L_s and $\dot{\phi}$ are the lead of the ball screw and its angular velocity. Also, the linear velocities in Y direction of the other grippers based on the time derivatives of the point displacements on the deployable scissor mechanism can be obtained as $v_{G_2} = -v_{G_5} = 3/5 v_{G_1}$ and $v_{G_3} = -v_{G_4} = 1/5 v_{G_1}$.

3.3 Singularity Analysis and Transmission Angle

The singularity analysis is a critical issue in parallel robots since the robot loses its controllability in singular configurations. To carry out such analysis, the singularity of Jacobian matrices must be studied. The direct kinematic singularity (second type) occurs whenever $|J_1| = 0$ while inverse kinematic singularity (first type) occurs whenever $|J_2| = 0$. The third type of singularity which is the combined singularity occurs whenever $|J_1| = 0$ and $|J_2| = 0$. Examining those Jacobian matrices reveals that when \mathbf{w}_i is along or coincident with \mathbf{u}_i for $i=1, 2$, direct kinematic singularities take place, while when \mathbf{w}_1 coincides with \mathbf{w}_2 , inverse kinematic singularities occur.

It is considerably to note that, for Delta robot, the direct kinematic singularity is related to the transmission angle β_i for $i=1, 2$ shown in Fig. 4(b). Namely, four singular configurations occur for β_i equals to zero or π for $i=1, 2$. From the geometry of

Fig. 4(b), the force transmission angle β_i can be obtained as follows

$$\beta_i = \arccos\left(\frac{1}{2l_1 l_2} |l_1^2 + l_2^2 - (\text{sgn}(i)e - x) - z^2|\right) \quad \text{for } i=1, 2 \quad (8)$$

In order to have high force transmission, the transmission angle $\beta_{\min} \geq \beta^*$ where $\beta^* = 35^\circ$ and $\beta_{\min} = \min(\beta_{1\min}, \beta_{2\min})$ (Huang et al, 2004).

3.4 Workspace Analysis

Two different types of workspaces are considered here, the achievable workspace and the objective one. The achievable workspace is based on the Delta robot construction while the objective workspace is based on the required transplanting task.

3.4.1 Achievable Workspace

The achievable workspace of the translational Delta robot in the X-Z plane is defined as the region in this space that can be reached by its end-effector. Carful inspection of the inverse kinematic solution (2) reveals that, the condition $F_i \leq 0$ for $i=1, 2$, should be hold in order to have real solution, where

$$F_i = Z_i^2 - 4l_i^2 (Z_i - (l_1^2 - l_2^2)) \quad \text{for } i=1, 2 \quad (9)$$

in which

$$Z_i = (x^2 + z^2 + e^2 + l_1^2 - l_2^2 - 2\text{sgn}(i)e x) \quad (10)$$

It can be proven that, (9) represents the equation of two concentric circles in X-Z plane, which represents the boundary of the achievable workspace as shown in Fig. 5.

3.4.2 Objective Workspace

Based on the transplanting cycle discussed above, the end-effector path during this cycle can be described as $P_0-P_1-P_2-P_1-P_0-P_3-P_0$ from which the regular objective workspace can be considered as a rectangle with vertices of $W_i(x_i, z_i)$ for $i=1\dots, 4$ as shown in Fig. 3. From the ergonomics point of view, the vertices $W_1(-40, -60)$, $W_2(-40, -115)$, $W_3(50, -115)$ and $W_4(50, -60)$ in cm shown in Fig. 3 are

considered. Figure 5 illustrates the overlapped of the objective workspace and the achievable workspace.

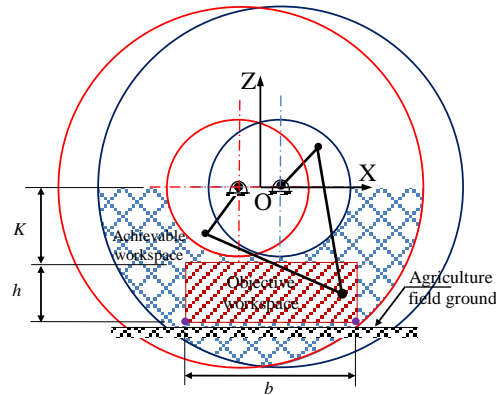


Figure 5: The achievable and the objective workspaces.

4 OPTIMAL DIMENSIONAL SYNTHESIS

The optimal dimensional synthesis is applied here for the Delta robot to obtain the optimal dimensions of its design parameters. Different objective functions either local or global for parallel manipulators are proposed in literature (Huang, T., et al 2004; Assal, S. F. M., 2017). Here, since the objective workspace of the proposed device is a specific workspace of a rectangle with known vertices, then the optimal dimensional synthesis is carried out here based on satisfying a prescribed workspace.

The objective function is a function that describes the achievable workspace that includes the objective workspace. Since the achievable workspace is given in (10) as $F_i = 0$ for $i=1, 2$, while the objective workspace is given by vertices points $W_j(x_j, z_j)$ for $j=1, \dots, 4$, then the objective function based on the power of point method [Laribi, M.A., et al 2007] is given as follows

$$O_f = \sum_{j=1}^4 \sum_{i=1}^2 |F_i(W_j, P)| \quad (11)$$

in which $P = (l_1, l_2, e)$ is the design parameters space.

Additionally, some kinematic constraints should be achieved; namely, high force transmission and avoiding forward kinematic singularities should be satisfied. In order to have high force transmission,

then $\beta_{\min} \geq \beta^*$ where $\beta_{\min} = \min(\beta_{1\min}, \beta_{2\min})$. From (8) this condition is equivalent to

$$C_1 = l_1^2 + l_2^2 - 2l_1 l_2 \cos \beta^* - K^2 \leq 0 \quad (12)$$

On the other hand, the forward kinematic singularities avoidance that is related to the force transmission angle can be achieved as $\beta_{\max} \leq \pi$ where $\beta_{\max} = \max(\beta_{1\max}, \beta_{2\max})$. Careful inspection of (8) reveals that this condition is equivalent to the following condition

$$C_2 = l_1^2 + l_2^2 - 2l_1 l_2 \cos(\pi) - (K + h)^2 - (e + b/2)^2 \geq 0 \quad (13)$$

Furthermore, in order to have enough space for mounting the two servo motors, the following constraint should be hold

$$C_3 = e - 10\text{cm} \geq 0 \quad (14)$$

In summary, the optimal dimensional synthesis is optimize the function $O_f(P)$ subjected to the constraints (12-14) to obtain the optimal $P^* = (l_1^*, l_2^*, e^*)$. The genetic algorithm (GA) toolbox of MATLAB is used to solve such optimization problem.

5 FINITE ELEMENT ANALYSIS

The finite element analysis (FEA) is used to carry out structural analysis. Structural analysis is the measure of how physical structure of a device and its components resist the deformation under certain loading conditions. The FEA of the proposed robot is carried out using ANSYS 17.2 version to investigate the effect of applied loads on the proposed robot at its worst case loading configuration. The configuration at which the proposed robot inserts its grippers into the growing tray to pick up the seedlings is the worst load configuration. This configuration takes place during the fetching phase and exactly at point P_2 . At this configuration, the inserting force per each gripper is 14 N, while the picking up force is 1 N per seedling (Kang et al, 2012). The obtained results from this analysis are then assessed to verify the suitability and the safety of the proposed robotic structure for the application. The steps for performing structural

analysis using ANSYS for the proposed robot are described as follows.

First, the Solid Works model of the proposed transplanter is exported into ANSYS Workbench. After having the proposed transplanter geometry defined, the Aluminium alloy material is selected and assigned to all parts of the multi-gripper scissor mechanism and the links of the two Diamond Delta robots, while Steel material is assigned to the rest of the components as illustrated in Table 1. The contact joints are assigned as well at this stage.

The adaptive meshing of the virtual prototype is then carried out. So, several trials are performed to improve the accuracy of the final results. After several trials, a mesh size of 10 mm is chosen and used. This meshing size gives better meshed structure with less computational time and cost than those of the values greater than or below 10 mm. The number of nodes and elements generated in this case are 643830 and 356630, respectively.

After the adaptive meshing, the boundary conditions are then applied. Namely, the bidirectional ball screw and sliders are fixed at both ends. Furthermore, a constant insertion force of 14 N in positive Z-direction is assigned to each of the 6 grippers that fixed at the scissor mechanism for the worst case loading configuration.

After applying the boundary conditions and loads, the deformations in X, Y, and Z- directions, total deformation and Von Mises Stress analyses are carried out.

Table 1: Material properties.

Material	Young's Modulus	Poisson's ratio	Density
Steel	200 GPa	0.3	7850kg/m ³
Aluminium	71 GPa	0.33	2700kg/m ³

6 RESULTS AND DISCUSSION

The optimal dimensional synthesis stage is carried out using the GA toolbox of MATLAB and yields $l_1 = 400$ mm, $l_2 = 921$ mm and $e = 120$ mm. Based on those link dimensions, the 3D model of the proposed robot is developed using Solid Works to be imported in ANSYS software for structure analysis as described in Section 5.

The FEA of the proposed transplanter is carried out using ANSYS at the worst case loading configuration and the results are presented here. The meshing of the constrained virtual prototype of the proposed transplanter is illustrated in Fig. 6. The deformations in X, Y and Z directions are depicted

in Figs 7, 8 and 9. It can be noted that, the maximum deformations in X, Y and Z directions are 0.044 mm, 0.0139 mm and 0.1482 mm, respectively. Additionally, the maximum total deformation of 0.1866 mm occurs in the middle of the scissor mechanism as illustrated in Fig. 10, which is quite acceptable.

Furthermore, the Von Mises stress is carried out to check whether the proposed transplanter is safe under the worst case loading condition. The results of Von Mises stress is shown in Fig.11. It can be pointed out that, the maximum Von Mises stress occurs at the ends of bidirectional ball screw and sliders. The maximum Von Mises stress is recorded as 43.186 MPa. Since the maximum allowable strength of the Aluminium alloy and the Steel materials considered for the transplanter parts are 280 MPa and 460 MPa, respectively, then the transplanter is shown to be safe with high factor of safety.

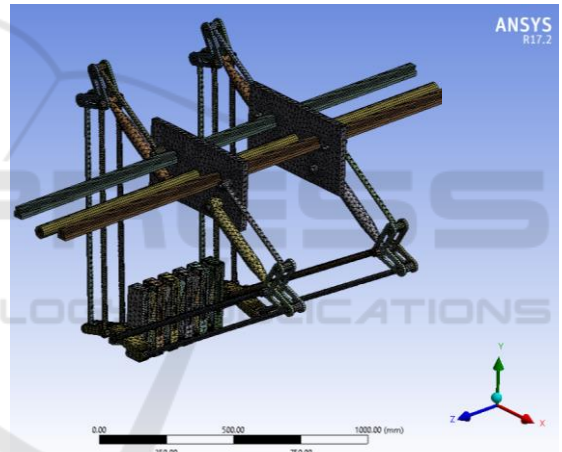


Figure 6: ANSYS meshing of the proposed transplanter.

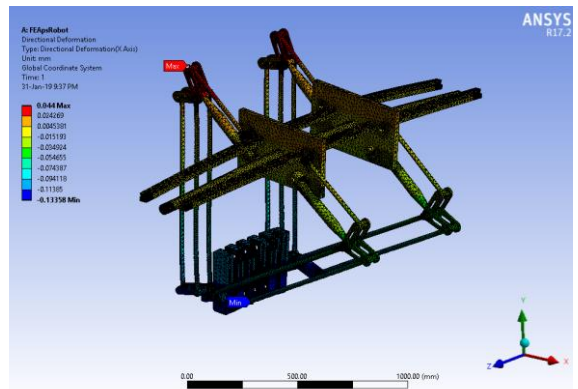


Figure 7: Deformation in X-direction.

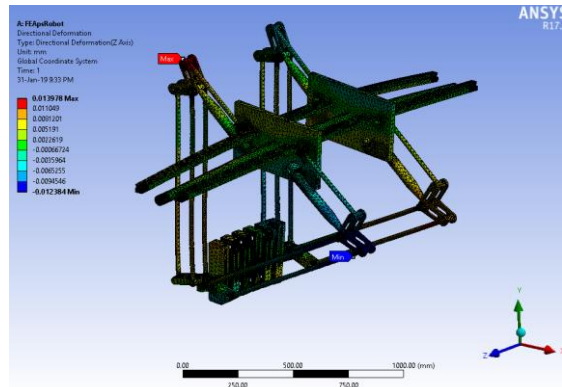


Figure 8: Deformation in Y-direction.

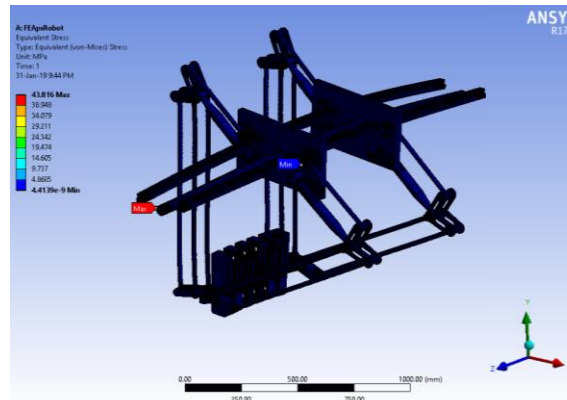


Figure 11: Von Mises stresses.



Figure 9: Deformation in Z-direction.

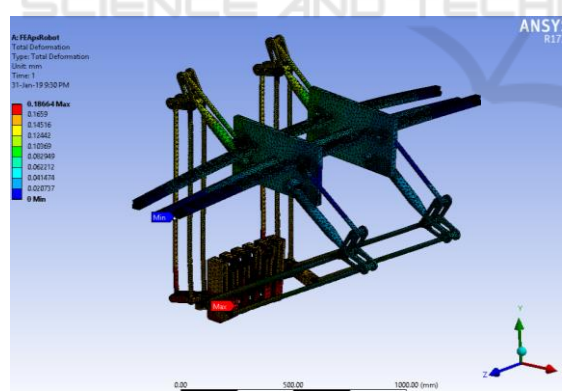


Figure 10: Total deformation.

7 CONCLUSIONS

A novel multi-gripper 3-DOF translational robot for row-by-row pot seedlings transplanting in the open agriculture field is introduced. It is based on hybrid parallel-deployable structure that enables seedlings transplanting from high dense distribution in a tray to low dense distribution in the open agriculture field in a row-by-row manner to increase the transplanting rate. The optimum design as well as the finite element analysis in the most critical loading configuration of the proposed transplanter is carried out. The FEA results prove that the proposed robot is safe in terms of stresses and deformations. Dynamic analysis and controller design as well as prototype fabrication are the future extension of this work.

REFERENCES

- Hwang, H., Sistler, F. E., 1986. A Robotic Pepper Transplanter, *Appl. Eng. Agric.*, vol. 2, no. 1, pp. 2-5.
 Kutz, L. J. , Miles, G. E. , Hammer, P. A. and. Krutz, G. W, 1987. Robotic Transplanting of Bedding Plants, *Transactions of the ASAE*, vol. 30, no. 3, pp. 586-590.
 Tmg, K. C., Giacomelli, G. A., and Shen, S. J., 1990. robot workcell for transplanting of seedlings part I - layout and materials flow, *Transactions of the ASAE*, vol. 33, no. 3, pp. 1005-1010.
 Hu, J., Yan, X., Ma, J., Qi, C., Francis, K. and Mao, H., 2014. Dimensional synthesis and kinematics simulation of a high-speed plug seedling transplanting robot, *Comput. Electron. Agric.*, vol. 107, pp. 64-72.
 Sakaue, O. 1996. Development of seeding production robot and automated transplanter system, *Japan Agricultural Research Quarterly*, vol. 30, pp. 221-226.

- Ryu, K. H., Kim, G. and Han, J. S., 2001. AE-Automation and Emerging Technologies: Development of a Robotic Transplanter for Bedding Plants, *J. Agric. Eng. Res.*, vol. 78, no. 2, pp. 141-146.
- Kang, D. H., Kim, D. E., Lee, G. I., Kim, Y. H., Lee, H. J. and Min, Y. B., 2012. Development of a Vegetable Transplanting Robot," *J. of Biosystems Eng.*, vol. 37, no. 3, pp. 201-208.
- Tian, S., Lichun Qiu, L., Kondo, N., Yuan, T., 2010. Development of automatic transplanter for plug seedling," *IFAC Proceedings Volumes*, vol. 43, no. 26, pp. 79-82.
- Xin, J., Kaixuan, Z., Jiangtao, J., Hao, M., Jing, P., and Zhaomei, Q., 2019. Design and experiment of automatic transplanting device for potted tomato seedlings, *Proceedings of the Institution of Mechanical Engineers, Part C: Journal of Mechanical Engineering Science*, vol. 233, no. 3, pp. 1045-1054.
- Jin, X., Li, M., Li, D., Ji, J., Pang, J., Wang, J. and Peng, L., 2018. Development of automatic conveying system for vegetable seedlings, *EURASIP Journal on Wireless, Communications and Networking*, vol. 2018:178, pages 1-9.
- Han, L., Mao, H., Hu, J. and Tian, K., 2015. Development of a doorframe-typed swinging seedling pick-up device for automatic field transplantation, *Spanish Journal of Agricultural Research*, vol. 13, no. 2, e0210, 14 pages.
- Xin, J., Kaixuan,Z., Jiangtao, J., Xinwu, D., Hao, M., and Zhaomei, Q, 2018. Design and implementation of Intelligent transplanting system based on photoelectric sensor and PLC, *Future Generation Computer Systems*, vol. 88, pp. 127-139.
- Tsuga, K., 2000. Development of fully automatic vegetable transplanter. *JARQ, Japan Agricultural Research Quarterly*, vol. 34, no. 1, pp. 21-28.
- Kumar, G. V. P. and Raheman, H., 2011. Development of a walk-behind type hand tractor powered vegetable transplanter for paper pot seedlings, *Biosyst. Eng.*, vol. 110, no. 2, pp. 189-197.
- Dihingia, P. C. Kumar, G. V. P. , Sarma, P. K. and Neog, P. 2018. Hand-Fed Vegetable Transplanter for Use with a Walk-Behind-Type Hand Tractor, *International Journal of Vegetable Science*, vol. 24, no. 3, pp. 254-273.
- Ndawula, I., Assal, S. F. M., 2018. Conceptual Design and Kinematic Analysis of a Novel Open Field 3DOF Multi Gripper Pot Seedlings Transplanting Robot, in *Proc. of the IEEE Int. Conf. on Mechatronics and Automation (ICMA 2018), Changchun, China, August 5-8*, pp.1458-1463.
- Huang, T., Li , Z., Li, M., Chetwynd, D. G., Gosselin, C. M., 2004. Conceptual design and dimensional synthesis of a novel 2-dof translational parallel robot for pick-and-place operations, *ASME Journal of Mechanical Design*, vol. 126, pp. 449-455.
- Kang, D. H., Kim, D. E., Lee, G. I., Kim, Y. H., Lee, H. J. and Min, Y. B., 2012. Development of a vegetable transplanting robot, *J. of Biosystems Eng.*, vol. 37(3), pp. 201-208.
- Assal, S. F. M., 2017. A novel planar parallel manipulator with high orientation capability for a hybrid machine tool: kinematics, dimensional synthesis and performance evaluation, *Robotica*, vol. 35, pp. 1031-1053.
- Laribi, M.A., Romdhane, L., Zeghloul, S., 2007. Analysis and dimensional synthesis of the DELTA robot for a prescribed workspace, *Mechanism and Machine Theory*, vol. 42, pp. 859-870.